Numerical Analysis of Nanofluidic Sample Preconcentration in Hydrodynamic Flow

Y. Wang*, K. Pant*, ZJ Chen*, W. Diffey**, P. Ashley**, and S. Sundaram*

*CFD Research Corporation, Huntsville, AL, U.S.A., yxw@cfdrc.com
**U.S.Army RDECOM, Redstone Arsenal, AL, USA

ABSTRACT

The phenomenon of sample enrichment due to the presence of an electric field barrier at the micro-nano-channel interface can be harnessed to obtain sample preconcentration that enhances sensitivity and limit-of-detection in sensor instruments. This paper presents a high-fidelity numerical analysis of the electrokinetics at the micro-nano-interface under pressure driven flows. Parametric analysis is performed to capture the critical effect of pressure head and background electrolyte (BGE) ion concentration on the electrokinetic and species transport of the preconcentrator. Our studies demonstrate that ion-polarization and electric field barrier can be established at micro-nano-channel interfaces and substantial sample enrichment (>10^4–fold) can be readily achieved using hydrodynamic flow. The results can be used for practical design and operational protocol development of novel nanofluidics-based sample preconcentrators.

Keywords: Nanofluidic, preconcentration, multi-physics

1 INTRODUCTION

Sample preconcentration is recognized as one of the most critical steps in high-performance, integrated lab-on-chip systems. Among various methods currently in use, nanochannel ion-polarization enabled by externally applied electric fields [1,2] or pressure gradients [3] hold great promise due to its capability for obtaining ultra-high enrichment ratios (up to 10^7–fold [1]). Several researchers have reported on experimental studies of nanochannel preconcentration without rigorous analysis to develop a fundamental understanding of the phenomenon. This paper presents the first, high-fidelity numerical study of nanofluidics-based sample preconcentration in hydrodynamic flows. Our analysis shows that both pressure and background electrolyte (BGE) concentration markedly impact the electrokinetics at the micro-nano-channel interface by varying the equilibrium of the species transport therein. Substantial analyte enrichment (>10^4–fold) can be achieved using nanofluidic preconcentrators. The modeling framework presented in this paper and our findings can be utilized to guide design and protocol development of sample preparation and biodetection technologies.

2 METHODS

2.1 Nanofluidic Preconcentrator

Figure 1 illustrates the geometry and principle of the nanofluidic preconcentration in hydrodynamic flow. A negatively charged nanochannel bridges two microchannels (or micro-reservoirs). A pressure head (Δp relative to the outlet) is applied at the inlet, transporting background electrolyte (BGE) ions and sample analytes towards the nanochannel. Due to the overlapping electric double layer (EDL) and unipolar nature of the nanochannel, a substantial electric field barrier is induced at the micro-nano interface, which precludes the negatively charged sample analytes from entering the nanochannel. As BGE carrying the analyte continuously flows through the channel, the analyte is enriched at the interface. To achieve adequate analyte enrichment in a reasonable processing time, strong electric field barrier and fast hydrodynamic flow are desired.

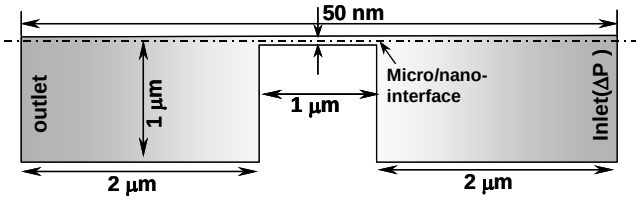

Figure 1. Schematic of nanofluidic preconcentrator.

2.2 Computational Models

Simulations are carried out using CFDRC-developed high-fidelity, multi-physics simulation environment, CFD-ACE+, in which three key modules – fluid flow, electric, and chemistry – were invoked to describe the fluid flow, electric field, and species distribution, respectively. A mathematical description of the models is presented next.

2.2.1 Electrostatic Models

The electric potential and field is governed by Poisson equation

$$\varepsilon_0 \varepsilon_r \nabla^2 \phi + F \sum_i z_i c_i = 0 \qquad (1)$$

where ε_0 and ε_r are, respectively, the electrical permittivity in the vacuum and the relative permittivity; F is the Faraday constant; z_i is the valence and c_i is the molar concentration of the i^{th} ionic species.

2.2.2 Species Transport Models

The species transport in the micro- and nano-channels is described by [4]

$$\frac{\partial c_i}{\partial t} + \nabla \cdot J_i = 0 \qquad (2)$$

Here the flux J_i of the i^{th} species is given by Poisson-Nernst-Planck (PNP) equation

$$J_i = -D_i \nabla c_i + u c_i + \omega_i z_i E c_i \quad (3)$$

where the terms on the R.H.S. respectively denote the species flux contributions from molecular diffusion, convection, and electromigration; ω_i is the electrophoretic mobility; D_i is the diffusivity; u is the velocity vector and $E = -\nabla \phi$ is the electric field. Note that Eq. (3) applies to both BGE ions and analytes. The flow of electrical current is a result of the individual flux of BGE ions in the solution, which is given by

$$I_i = F z_i J_i = F\left(-z_i D_i \nabla c_i + u z_i c_i + \omega_i z_i^2 c_i E\right) \text{ and}$$
$$I_{tot} = \sum_i I_i = F \sum_i z_i J_i \quad (4)$$

The three terms on the R.H.S of the first equation signify the current contributions from diffusion, convection, and electromigration of the i^{th} species, respectively. It should be mentioned that while there is no overall current (I_{tot}) in the hydrodynamic case, the current component of the i^{th} (I_i) BGE ion can be non-zero.

2.2.3 Fluidic Models

Viscous, incompressible fluid flow in the micro- and nano-channels is described by the conservation of mass and momentum equations [4]:

$$\frac{\partial u}{\partial t} + (u \cdot \nabla)u = \mu \nabla^2 u - \nabla p / \rho + f_e \quad (5)$$
$$\nabla \cdot u = 0$$

where u, ρ, μ, and p are the fluid velocity, density, dynamic viscosity, and pressure respectively; f_e is the electrostatic body force due to the electrostatic charges (Columbic force) and is expressed as

$$f_e = EF \sum_i z_i c_i \quad (6)$$

2.3 Simulation Methods

As the preconcentrator is normally used to address the analyte at the trace-level concentrations (pico–nano molar), we will assume that the analyte is so dilute that their presence does not alter the electric field, flow, and BGE ionic equilibrium. Following the regular perturbation analysis of Bharadwaj and Santiago [5], our simulation is conducted in two steps. In the first step, Eqs. (1), (2), and (5) are solved in a coupled manner to resolve the flow (u), electric field (E), and BGE ion concentrations (c). In the second step, Eq. (2) is solved for the analyte with u and E from the first step. This approach is most suitable for dilute analyte concentrations, which is typical for a variety of proteomic, genomic, and chemical compound analysis.

Boundary conditions are also supplied for closure of the equations. Electrically, zero potential and zero surface charge density (i.e., zero electric field) are applied at the outlet and the inlet, respectively. A fixed surface charge density (–0.002 C/m^2 [4]) is specified at the nanochannel walls while charges on the microchannels are neglected. For BGE flow, a differential pressure is applied between the inlet and outlet. No-slip boundary conditions are invoked at all channel walls. For BGE ion transport, a constant bulk ion concentration is provided at both the inlet and outlet. For the analyte, a constant concentration is set only at the microchannel inlet. Table 1 lists all the relevant parameters used in the simulation, where KCl is used as the BGE. Given the simulation parameters, Eq. (4) can be simplified as

$$I_{tot} = F\left(-D\nabla\left(c_K - c_{Cl}\right) + u\left(c_K - c_{Cl}\right) + \omega\left(c_K + c_{Cl}\right)E\right) \quad (7)$$

For sake of brevity, a single diffusivity D and mobility ω are used for both K and Cl in Eq. (7). A fully structured computational domain consisting of ~17,000 cells was generated for the entire preconcentrator. Grid checks were performed to ensure mesh-independent results. Specifically, 61×51 grid points in a power law distribution were used to resolve the longitudinal and transverse dimensions of the nanochannel.

Table 1. Simulation parameters for numerical analysis

Case No.	1	2	3	4	5
Electrolyte Conc. (M)	10^{-4}	10^{-4}	10^{-4}	$2X10^{-5}$	10^{-3}
Pressure ΔP (atm)	0.1	0.2	0.4	0.2	0.2

3 RESULTS AND DISCUSSION

In the simulation analysis, case 2 is used as the baseline. The effects of pressure head and BGE ion concentrations are, respectively, captured by cases 1, 2, and 3, and cases 2, 4 and 5. Simulational results are used to interpret the field variation of the BGE and to evaluate sample preconcentrator performance.

3.1 Background Electrolyte

Figure 2 shows the contour plots of K^+ and Cl^- ion concentrations for the baseline case. Note that non-uniform ion concentration develops in the electric double layer (EDL) in the nanochannel. The concentrations of both ions at the two interfaces are different (i.e., ion-polarization [4]).

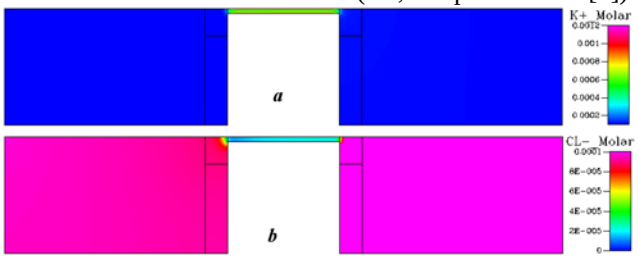

Figure 2. Contour plot of BGE ion concentrations.

Figure 3a shows the transverse profile of K^+ and Cl^- ion concentrations and indicates that a strongly overlapped EDL is established in the nanochannel. The EDL effect is more pronounced for low BGE concentrations and the channel is essentially filled with a unipolar solution of K^+,

viz., the solution is dominantly occupied by K^+ ions (note the logarithmic *y*-axis). Figure 3b displays the longitudinal profile of K^+ and Cl^- ion concentrations. In the microchannel, both remain almost constant to satisfy the electroneutrality, i.e., $\sum z_i c_i = 0$. In the nanochannel, the concentration of counter-ion (K^+) is appreciably higher than the co-ion (Cl^-) to neutralize the negative charges on the channel wall. As a result, steep gradients of the BGE ion concentrations form at the micro-nano interface.

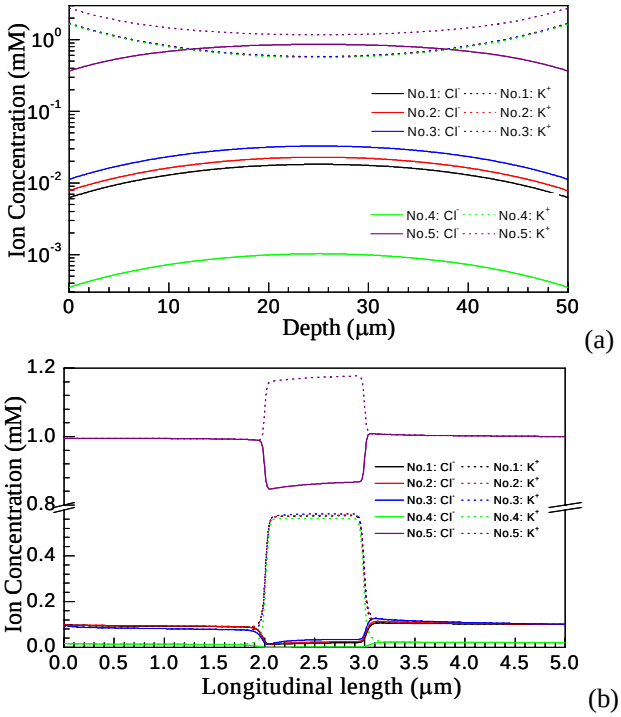

Figure 3. Profile of BGE ion concentrations. (a) Transverse (b) Longitudinal.

Figure 4 shows the pressure distribution along the channel centerline (dash-dot line in Figure 1). The pressure drop in the microchannel is negligible and is nearly linear in the nanochannel. Given the same pressure head (case No. 2, 4, and 5), the pressure drop in the nanochannel is larger for high BGE concentrations (case No. 5). This is attributed to the smaller EDL thickness and smaller concentration difference between K^+ and Cl^- ions at the micro-nano interface, both reducing the electrostatic body force that impedes flow.

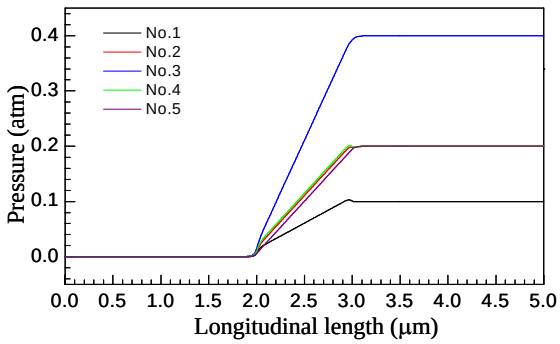

Figure 4. Longitudinal Pressure distribution

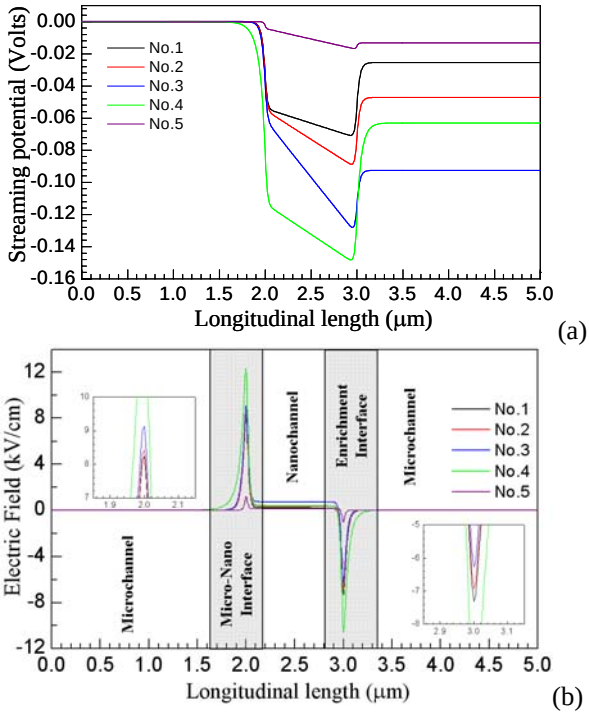

Figure 5. Longitudinal profile of (a) electric streaming potential and (b) electric field.

Figure 5a depicts the longitudinal dependence of the streaming potential and the electric field. The streaming potential is an electric potential generated by the directional movement of the non-electroneutral electrolyte under a pressure gradient through a channel [6]. A larger pressure head and lower electrolytic concentration yield a larger potential because of the increased flux of the non-electroneutral charges. A point of interest is that while the potential difference between the inlet and the outlet is small (0–0.1 Volts), the potential variation along the centerline is non-monotonic and *an abrupt drop/rise occurs at the interfaces, leading to strong electric fields for preconcentration.* This is distinctly different from previous observations on streaming potential (or field) in a single microchannel or nanochannel. The induced electric field (3rd term in Eq. (7)) counteracts the current contributions from molecular diffusion and convection (first two terms in Eq (7)). Figure 5b reveals that the entire nano-preconcentrator can be divided into five sub-domains: two microchannel (electroneutral) segments, nanochannel (non-electroneutral), and two micro-nano interfaces. In the microchannels, electroneutrality produces zero electric field (note I_{tot}=0 in Eq. (7)). In the nanochannel, the gradient of the BGE concentration is almost constant along the longitudinal direction, leading to negligible current contribution from molecular diffusion. Therefore, a constant electric field is induced to counteract the convection current. At the micro-nano-interface, the scenario is more complicated and the currents from diffusion, convection, and migration are all comparable. At the interface to the right (termed the enrichment interface),

NSTI-Nanotech 2008, www.nsti.org, ISBN 978-1-4200-8505-1 Vol. 3

the diffusive current flux points to the right (see Figure 3b) and needs to be balanced by combined convection and electromigration (to meet I_{tot}=0). Therefore, the electric field is directed to the left (i.e., negative) and its magnitude decreases with an increase in pressure head (viz. convection current becomes stronger), although the overall inlet-outlet potential difference increases. It is the electric field that serves as a barrier that repels negatively charged analytes that approach the interface and enables analyte enrichment. In contrast, at the interface to the left, ion diffusion aligns with convection (both pointing to the left) to oppose the electromigration-induced current (3rd term in Eq. (7)). Hence, the electric field points to the right (i.e., positive). For the same reason, the magnitude of the electric field at the left interface is higher than that at the right interface (see Figure 5b).

3.2 Sample Preconcentration

Figure 6 shows the transient evolution of enrichment ratio (ER) of four sample analytes (A-D) as well as the snapshots of analyte-B preconcentration at the enrichment interface on the right in case No. 3. ER is defined as the ratio of the highest analyte concentration in the computational domain to that at the inlet. The analytes have diffusivity $D_{A\text{-}D}$ = {1,2,4,1}×10^{-11} m^2/s and mobility $\omega_{A\text{-}D}$ = {2,2,2,1}×10^{-11} m^2/(sV). Our results suggest that ER depends strongly on analyte properties (in particular, mobility). A large electrokinetic mobility results in a stronger electromigration force leading to a higher ER. Depending on analyte properties, ER>10^{4}X can be successfully achieved.

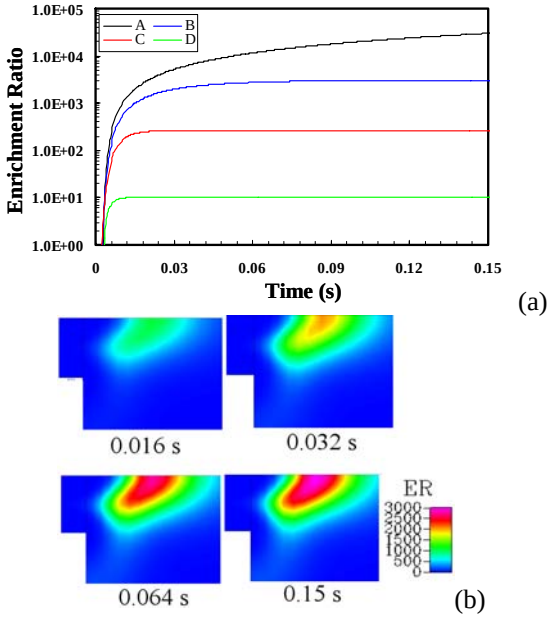

Figure 6. Transient evolution of Enrichment ratio of four sample analytes and contour plot for analyte-B in case No. 3.

Our simulation results (not shown) also indicate that at smaller pressure heads, ER for an analyte reaches a much higher value but at a slower pace (longer enrichment times). This is due to the fact that lower pressure head (or slower flow velocity) reinforces electric field barrier at the enrichment interface while attenuating the convection force that pushes the analyte through the nanochannel.

4 CONCLUSION

In this paper, we have investigated the electrokinetics of a nanofluidic hydrodynamic sample preconcentrator. Multi-physics simulations, which solve the electric field, fluid flow, and species transport in a coupled manner, were carried out. Our analysis clearly demonstrates that a substantial electric field barrier is established at the micro-nano-interface and the equilibrium of electrolytic ion transport is significantly impacted by the pressure head (or pumping flow) and background electrolyte concentration, which can be employed for the development of effective sample preconcentration technologies. Depending on the current flux characteristics, the entire preconcentrator can be divided into five sub-domains. In the microchannel domain, current flux due to diffusion, convection, and electromigration are negligible. In the nanochannel, the longitudinal diffusion is negligible and, the convection-induced current flux is balanced by the electromigration. In the micro-nano interface, all current contributions are important and the diffusion-induced current carries a considerable weight in determining the direction and magnitude of the electric field therein. An interesting point of note is that the field strength in the barrier decreases with increasing pressure head (or pumping flow) and electrolytic concentration (i.e., thinner EDL). Therefore, a tradeoff exists between the enrichment ratio and operating time, which needs to be addressed in practical design and protocol development. Our analysis has also revealed that the enrichment ratio also relies heavily on analyte properties (e.g., mobility and diffusivity of the analytes) and substantial (>10^4–fold) analyte enrichment can be readily achieved.

ACKNOWLEDGEMENT

This research is sponsored by the DARPA and US Army Aviation & Missile Command under grant number W31P4Q-07-C-0035.

REFERENCES

[1] Y.C. Wang *et. al*, *Anal.Chem.*, 77, 4293-4299, 2005.
[2] S.M. Kim *et. al*, *Anal.Chem.*, 78, 4779-4785, 2006.
[3] A. Plecis et al., Proc. MicroTAS'2005, 2, 1038-1041, 2005.
[4] H. Daiguji *et. al*, *Electrochem. Commu*, 8, 1796-1800, 2006
[5] R. Bharadwaj and JG. Santiago. *J. Fluid Mech.* 2005, 543, 57-92.
[6] RF Probstein. An Introduction to Physicochemical Hydrodynamics. John Wiley & Sons, 2nd Ed. 1995.